The Fluorescence Intermittency for Quantum Dots Is Not Power-Law Distributed: A Luminescence Intensity Resolved Approach

Robert Schmidt,† Cornelius Krasselt, Clemens Göhler, and Christian von Borczyskowski*

Institute of Physics, Optical Spectroscopy and Molecular Physics, Centre for Nanostructured Materials and Analytics (nanoMA), Technische Universität Chemnitz, 09107 Chemnitz, Germany. The manuscript was written through contributions of all authors. All authors have given approval to the final version of the manuscript.
†Present address: Ultrafast Solid-State Quantum Optics and Nanophotonics, Münster University, 48149 Münster, Germany

ABSTRACT The photoluminescence (PL) of single emitters like semiconductor quantum dots (QDs) shows PL intermittency, often called blinking. We explore the PL intensities of single CdSe/ZnS QDs in polystyrene (PS), on polyvenylalcohol (PVA), and on silicon oxide (SiO_x) by the change-point analysis (CPA). By this, we relate results from the macrotime (sub-ms to 1000 s) and the microtime (0.1−100 ns) range to discrete PL intensities. We conclude that the intensity selected "on"-times in the ms range correspond to only a few (discrete) switching times, while the PL decays in the ns range are multiexponential even with respect to the same selected PL intensity. Both types of relaxation processes depend systematically on the PL intensity in course of a blinking time trace. The overall distribution of on-times does not follow a power law contrary to what has often been reported but can be compiled into 3−4 characteristic on-times. The results can be explained by the recently suggested multiple recombination centers model. Additionally, we can identify a well-defined QD state with a very low PL intensity above the noise level, which we assign to the strongly quenched exciton state. We describe our findings by a model of a hierarchical sequence of hole and electron trapping. Blinking events are the consequence of slow switching processes among these states and depend on the physicochemical properties of the heterogeneous nanointerface of the QDs.

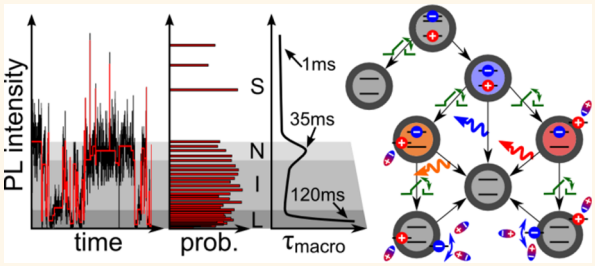

KEYWORDS: photoluminescence intermittency · single quantum dots · change point analysis · multiple recombination centers · spectral diffusion · photoluminescence decay · CdSe/ZnS

The detection and spectroscopy of single nanoscopic emitters reveals unique electronic and optical properties as compared to the corresponding ensemble. One fundamental feature is the photoluminescence (PL) intermittency,[1] also called "blinking", which is observed for many nanoscopic emitters[2−6] like semiconductor quantum dots (QDs), single molecules, fluorescent proteins or metallic nanocrystals[7] and even defect centers in diamond nanocrystals.[8] It is a very general observation that blinking is closely related to (structural and/or energetic) disorder,[2,8] as it is, for example, present in polymer matrices and at (strained or multicomponent) interfaces. In most cases the PL is divided into dark "off"- and bright "on"-states, but especially for QDs also "dimmed" or "grey" (intermediate) intensities are observed.[9] In case of QDs and some dye molecules, dynamics of off- and on-events are reported to follow a broad range both in time (hundreds of microseconds up to hours) and probability density of the related occurrence.[2−6] Furthermore, the corresponding probability distributions for on- and off-times are often described by (truncated) power laws.[2−6] The experimentally reported power law behavior, however, is not immediately evident for on-times, since even if many acceptor states are simultaneously accessible for an initially excited state the decay rate should be the sum of all (parallel) decay rates.

Though many experiments and several models deal with blinking phenomena, their explanation is under strong debate even after two decades. Several models were proposed.[2−6,10−16] Recent experiments on CdSe/CdS QDs questioned the

* Address correspondence to borczyskowski@physik.tu-chemnitz.de.

Received for review December 23, 2013 and accepted February 28, 2014.

Published online March 01, 2014
10.1021/nn406562a

up to now favored long-time charging model, since the underlying Auger effects are obviously too small to result in effective PL quenching in that case. Additionally, states with very low PL intensities have been identified.[9,17−20] Very recently Amecke *et al.*[10] suggested that also large CdSe/ZnS QDs show evidence for the presence of such low intensity states.

New models explain blinking by fluctuations of nonradiative relaxation rates of the excitonic states. These models rely on the influence of multiple recombination centers (MRC).[21−23] A multitrapping model has been suggested by Ye *et al.* while also taking Auger processes into account.[24] Pelton *et al.*[25] have introduced a power spectral density approach to analyze blinking phenomena. This approach has been applied very successfully in the recent MRC model.[23] A comparison of predictions from this model with previous experimental findings provides strong evidence for a universality of the MRC model.[23] Clearly, these investigations show that the often reported power law behavior is one but not the only feature of blinking dynamics. Both, deviations from a power law and the strong influence of the environment on blinking dynamics have been shown in our lab.[14−16,26,27]

Contrary to the power spectral density approach, almost all experiments identify on- and off-times by setting an intensity threshold somewhat above the background. This may cause artifacts and influence systematically the often identified truncated power law.[28] Moreover, this approach does not discriminate between on- and dim- (grey) intensities. The promising developments related to MRC stimulated us to further explore QDs beyond the conventionally applied on−off analysis to find more experimental evidence for the most adequate blinking model. To overcome the simplifying experimental approach of setting a constant threshold, we make use of a recently developed analytical tool, the change-point analysis (CPA).[29] This method not only takes on- or off-PL intensities into account, but also can handle the rich features of intermediate intensities.

To go further beyond blinking statistics and to understand the physical background of QD blinking, it is essential to relate the dynamics in the intensity domain (intermittency) to those in the time and spectral domain. PL decay dynamics show, for example, a pronounced nonexponential behavior both for ensembles[30−34] and single QDs.[35−39] In this study, we report that CPA provides means to investigate simultaneously the dynamic of both on- and off-times, PL decay times, and spectrally resolved features in detail. Moreover, also a relation to spectrally resolved features will be reported. The present study is therefore not a detailed extension of numerous previous reports on blinking phenomena in various quantum systems, but aims at a basic understanding of the underlying physical processes of the blinking statistics, especially of on-times. We interpret our results in the spirit of the MRC approach and present a hierarchical model of switching between exciton, hole, and electron states. Switching times show a narrow distribution, which is against an interpretation by a power law.

RESULTS

Throughout the paper we will present experimental data for a single, but sometimes different CdSe/ZnS QDs (numbered for recognition and comparison) to give an impression how experimental features vary from QD to QD. Altogether we investigated about 60 CdSe/ZnS QDs in 3 different matrices, namely, in polystyrene (PS), on polyvenylalcohol (PVA), and on silicon oxide (SiO_x), which also affects some of the PL properties. Several examples and especially the results for QDs on PVA are given in the Supporting Information. The CPA-based identification of a (for a certain time) constant PL intensity allows for an intensity resolved analysis of QD blinking dynamics (see Methods for time resolution). Figure 1a,b shows typical subsets of a PL time trace of QD10 in PS with 1 ms binning time (black data and top panel in (b)) and the related on-intensities as determined by CPA (red line and bottom panel in (b)). CPA analysis results in intensity histograms, which provide information on not only distributions of intensity levels, but also their respective length, as will be discussed later. Figure 1c shows such an intensity histogram illustrating how often a specific intensity is realized during the total observation time of 15 min.

CPA can only identify constant intensities (inter-photon times) but not absolute ones since these depend on the absolute number of photons. By implication, the intensity identified during a short time lap depends on a small number of emitted photons and is less certain as compared to the one obtained during a long time lap. To overcome this problem, a clustering algorithm, also developed by Watkins *et al.*,[29] is applied. The respective intensity histograms before and after the clustering procedure, showing either continuously distributed or discrete (counted by index *n*) intensity levels, are compared in Figure 1c,d, respectively. The clustered histogram reveals that intensity levels are nearly equally distributed in occurrence, whereas the density of intensities changes according to the number of (nonclustered) intensity levels in the "classical" intensity histogram shown in Figure 1c.

It is evident from Figure 1d that there are 4 distinct regions of intensities. In this typical example we observe densely clustered intensities "L" at low intensities (<4 kcps), less dense clustered intermediate intensities "I" between 4 and 17 kcps, and normal ones "N" between 17 and 27 kcps. In the given example of CdSe/ZnS QD10 in PS the distribution of N-intensities is denser as compared to the one in the range I. Dense intensities N do not show up in all cases as can be seen for another QD in PS in Figure 2d (QD9). We have shown recently,[39] that the density of intensities N depends on the embedding matrix of the QDs and is

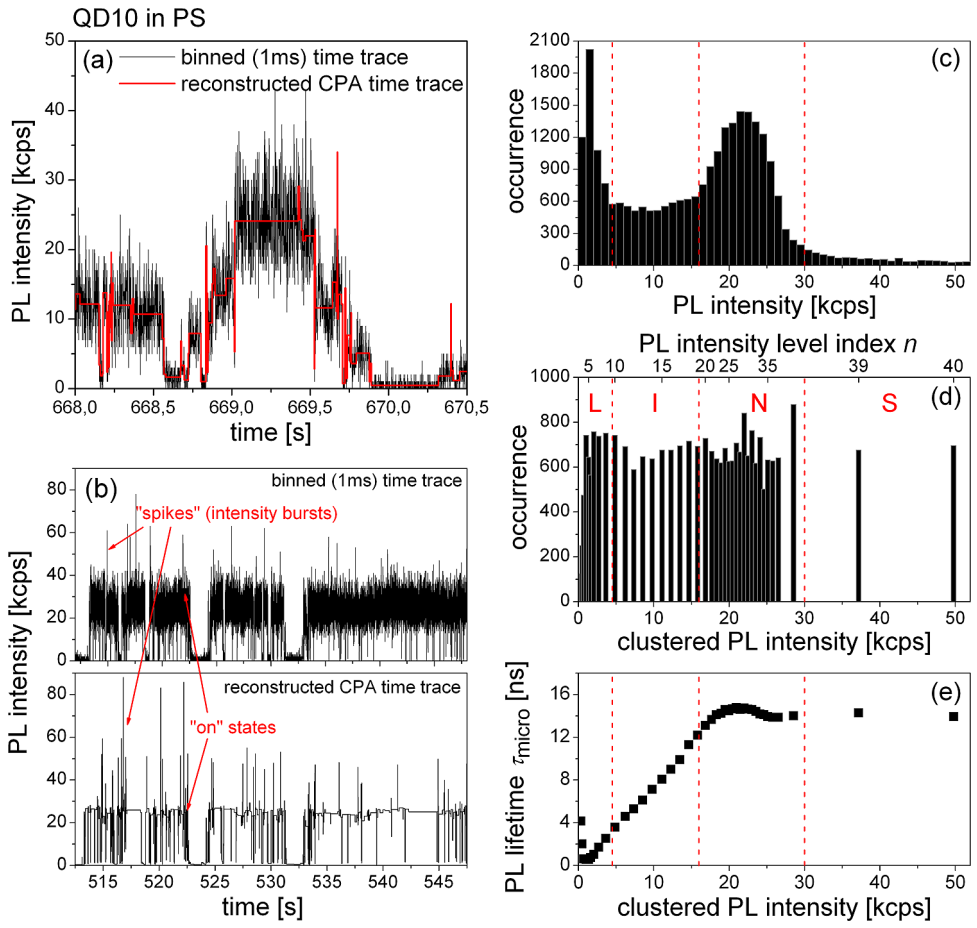

Figure 1. PL data of the exemplary single CdSe/ZnS QD10 in PS. (a) Subset of the PL intensity time trace with black and red data presenting the binned (integration time 1 ms) and CPA reconstructed time trace, respectively. The multi-intensity blinking as well as the reproduction of the binned time trace by CPA is clearly visible. (b) Long PL time trace of 1 ms binned (top) and CPA reconstructed (bottom) data. Strong intensity spikes are visible in both data sets for this QD in PS. (c,d) CPA histogram of constant intensities before (c) and after (d) PL intensity clustering. Besides the intensity given in kcps, we also indicate an intensity level index *n*. In this example of CdSe/ZnS on PVA a high density of intensities in the N-range is visible. This feature arises also for other but not all QDs in PS, whereas it is typical for QDs on PVA.[37] More examples are given in the Supporting Information. (e) PL lifetime as a function of clustered PL intensity of CdSe/ZnS on PVA. Data evaluation follows a monoexponential fit for simplicity. Deviations are detectable below $I \approx 15$ kcps (ranges L and I, see also Figure 3). Note that the data presented in the figures are obtained for different single CdSe/ZnS QDs in PS, on PVA or on SiO_x. The general features are very similar for all (about 60) QDs. For typical differences, see the Supporting Information.

in close relation to deviations from a truncated power law.[16] We therefore can assign each QD either to the class of dense or no-dense N-intensities. Details of this effect have been reported elsewhere[16,39] and will also be given in the Supporting Information.

We have included the PL decay time τ_{micro} in the ns range (approximated by a monoexponential fit) as a function of clustered intensities in Figure 1d. We note that the "overshoot" of the PL lifetime around I = 20 kcps is only observed for QDs with dense N intensities (see QD9 in Figure 2c,d for comparison).

Finally, at very high intensities we observe (isolated) spikes "S" between 30 and 50 kcps. To test whether these high intensities might stem from CPA artifacts, we compare in Figure 1b the (binned) real-time blinking time trace (top) with the corresponding CPA-based time trace shown below. Both diagrams show high (but very short) intensity spikes, which are detected only under the condition of very short (1 ms) binning times and might have been overlooked in many previous experiments.

Throughout the paper we will now concentrate on those QDs (in PS), which can be described in an analogous manner as QD9 shown in Figure 2, that is, the presence of a truncated power law according to eq 2 (see below) and (uniquely related to this) the near absence of dense N intensities. Other examples will be discussed in the Supporting Information or in the case that a comparison provides valuable information to set up an appropriate model of PL dynamics. Figure 2 comprises some relevant data, which characterize such a representative CdSe/ZnS QD in PS. It assembles a comparison of the (threshold-based) log−log presentation of on-time statistics (Figure 2a), a CPA-based clustered intensity histogram (Figure 2d), and related PL lifetimes τ_{micro} in the *microtime* range of ns, which have been

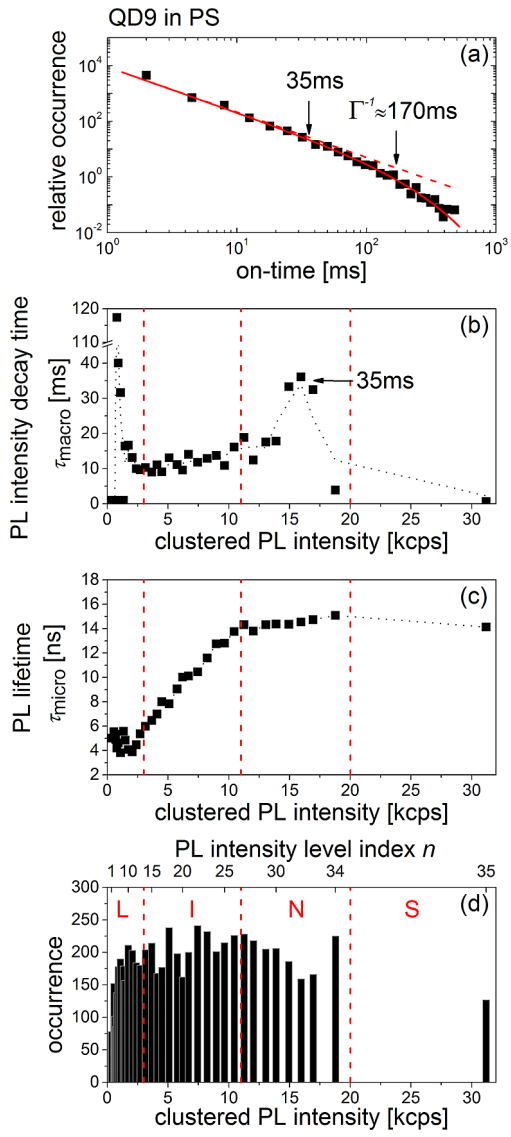

Figure 2. PL dynamic of the single CdSe/ZnS QD9 in PS. (a) Conventional (binned) on-time histogram and truncated power law analysis following eq 2 (red solid line). Both deviation from an exclusive power law (dashed line) at 35 ms and (exponential) truncation time $\Gamma^{-1} \approx 170$ ms are indicated. (b) Intensity decay times τ_{macro} as a function of the clustered intensity according to a monoexponential fit. Note the maximum of τ_{macro} at 35 ms which is also visible in (a). A further maximum shows up at very low PL intensities at $\tau_{macro} \approx 120$ ms, which approximately corresponds to the truncation time of the power law in (a) and will escape detection in a threshold based analysis. Typical intensity ranges (see text) are indicated by red dashed lines. (c) PL decay times τ_{micro} as a function of clustered intensities. The fits correspond to a monoexponential data treatment, which is only an approximation for intensities below $I \approx 15$ kcps (see Figure 3 for details). Typical intensity ranges are indicated. (d) Clustered PL intensity distribution with marked ranges of intensities (see text).

obtained assuming (for convenience) a monoexponential decay as a function of the clustered intensity (Figure 2c). Furthermore, we collect data for the long time decay τ_{macro} of the individual intensities in the *macrotime* range of ms in Figure 2b. τ_{macro} has been obtained by fitting the distribution of on-periods for each intensity identified by CPA. The basic findings shown in Figure 2 demonstrate that CPA allows discussing PL lifetimes τ_{micro} and on-times τ_{macro} in close relation to each other providing interdependent information for identical PL intensities. To simplify this obviously complex relationship, we first treat separately the two time regimes and discuss the interrelation of the two thereafter.

Microtime Scale (PL Decay Time τ_{micro}). Figure 2c shows the PL intensity-lifetime (τ_{micro}) relation. PL lifetimes τ_{micro} depend in a complex way on the PL intensity as is obvious from Figure 2c. In a first approximation the PL decay has been fitted for each intensity level by a monoexponential decay function. Since the PL lifetime τ_{micro} can be determined quite accurately because of the large number of photons (in the order of 10^5 counts) contributing to every PL intensity, distinct deviations from a monoexponential PL decay are readily observed. Two observations immediately emerge applying a detailed decay analysis (Figure 3, QD8 in PS), that is, a nonexponentiality at low (L) and intermediate (I) intensities and a constant lifetime τ_{micro} at high and very high intensities (N and S, respectively). For the latter ones, we observe a completely monoexponential decay. On the contrary, up to 3 exponential functions are needed to describe the PL decays adequately for the remaining PL intensities I and L. Let us first analyze the intensity ranges termed I and L in Figure 3 omitting intensities N and S for the moment.

The PL decay can be satisfactorily fitted by two exponential decay functions in the intermediate intensity range I. This implies that each intensity can be assigned to at least two different QD states characterized by the PL decay parameters (A_1, $\tau_{micro,1}$) and (A_2, $\tau_{micro,2}$), respectively. The related states must have different radiative (k_r) and nonradiative (k_{nr}) PL decay rates, since otherwise they cannot be assigned to the same PL intensity (except for the case of compensating population rates, which does not apply here; discussed below). The corresponding fitting parameters $\tau_{micro,i}$ and A_i are shown in Figure 3a,b. All decay times τ_{micro} are nearly identical for QDs both in PS and on PVA (see the Supporting Information). The lifetimes are in the range $\tau_{micro,1} \approx (7-14)$ ns and $\tau_{micro,2} \approx (2.5-5)$ ns. Both $\tau_{micro,i}$ increase nearly linearly with PL intensity in the range I. A linear relationship has been observed earlier[36,37] and can be explained by a simple model including radiative and nonradiative decay channels. With the assumption that the PL intensity I of an emitting state is proportional to its quantum yield QY and to the population rate k_{pop} into this state, it follows that

$$I \propto k_{pop} QY = k_{pop} \frac{k_r}{k_r + \sum_i k_{nr,i}} = k_{pop} k_r \tau_{micro} \quad (1)$$

Since $\tau_{micro,1} > \tau_{micro,2}$ (higher nonradiative rates for state 2) holds for each intensity $I = I_1 = I_2$, the relation $k_{pop,1}\ k_{r,1} < k_{pop,2}\ k_{r,2}$ follows immediately. Assuming

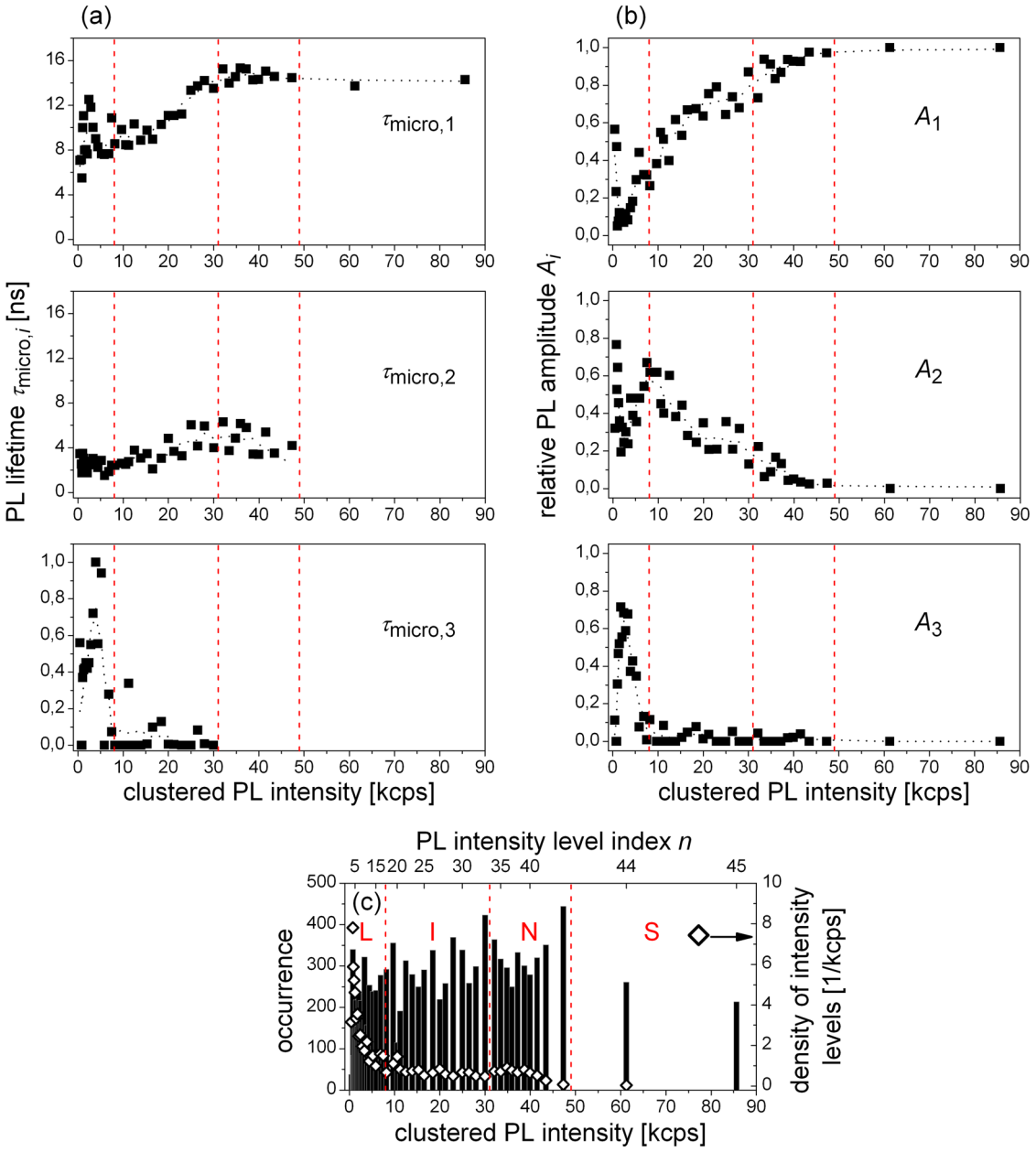

Figure 3. (a,b) Multiexponential fit of the PL decay of the single CdSe/ZnS QD8 in PS as a function of the clustered intensity I with decay times $\tau_{micro,i}$ (a) and corresponding (relative) amplitudes $A_i/(A_1 + A_2 + A_3)$ (b). Red dashed lines indicate intensity ranges given in (c). Black dotted lines correspond to data smoothing (5 adjacent point averages) and are merely a guide for the eye. (c) Corresponding occurrence of clustered PL intensities including marked intensity ranges. Diamonds correspond to the density of PL intensities indicating a high density in the range L and a slightly increased one in the range N. The level index n is also given on top of the graph.

similar radiative rates $k_{r,1} \approx k_{r,2}$, this leads to $k_{pop,2}/k_{pop,1} \approx \tau_{micro,1}/\tau_{micro,2} \approx 3$, *i.e.*, a higher population rate of state 2 (factor of about 3) compared with state 1, and also accounts for the different slopes (inverse of $k_{pop,i}\, k_{r,i}$) in the $\tau_{micro,i}$ relationships. $\tau_{micro,1}$ raises up to the highest intensities opposite to $\tau_{micro,2}$ (whose contribution A_2 obviously vanishes completely with the beginning of N intensities). This means that the underlying decrease of the nonradiative rates with increasing PL intensity is stronger for state 1, whereby it is for example fixed for state 2 on a certain minimum level. Alternatively, another state exists that emits at high PL intensities N (less strong nonradiative rate, higher population rate), exhibiting a PL lifetime indistinguishable to the one of state 1 at high PL intensities.

Figure 3 also reveals that an additional very fast PL decay time $\tau_{micro,3} \approx 1$ ns shows up in the low intensity range L. This component does not continuously grow-in with increasing intensity but is limited to a narrow intensity range. In a time integrated analysis such a short-lived component corresponds to a nearly off-intensity, although it is clearly above the background

intensity. This finding indicates the presence of a weakly emitting but short-lived state as has also been found recently for a somewhat larger CdSe/ZnS QD.[10]

Remarkably, the PL lifetime τ_{micro} is monoexponential and close to 14 ns in the intensity ranges N and S. It is independent of the PL intensity, though the intensity varies by more than a factor of 2 (see Figures 2c and 3). This finding is in strong contradiction to what is expected from eq 1 while assuming a constant population rate k_{pop} for all intensities. Especially, the observed PL spikes S (see Figures 1b,d, 2d, and 3c) are at first glance a puzzling observation. How can this be explained? In the present experiment CdSe/ZnS QDs were excited at 2.667 eV, which is about 380 meV above the respective absorption origin at 2.284 eV. Such an excitation occurs into higher electronic states. Knappenberger *et al.* have shown that on-time blinking dynamics depend on excitation wavelength at such elevated excitation energies.[40] This indicates that above a certain excess energy new pathways for nonradiative processes are opened by creating, for example, hot electrons. This implies also that absorption and PL excitation spectra do not coincide, as we have indeed observed experimentally in many cases for ensembles of a large variety of CdSe QDs. Recently, Galland *et al.* have shown that such alternative decay channels can be blocked by charging of otherwise accessible quenching trap states.[41] In case of blocking of such channels, excitation will completely proceed to the emissive state and will thus increase the PL intensity due to an increased population rate k_{pop} (see eq 1) without substantial influence on the PL decay time. CPA reveals that an effective blocking of such quenching channels is active for only very short times (see Figure 1b). To explain these findings, a possible excitation scheme is presented in Figure 4.

Macrotime Scale (On-Times t_{on} and τ_{macro}). Now we turn to the analysis of on-times. The probability density $p_{on}(t_{on})$ of (threshold-based) on-times t_{on} shown in Figure 2a seems to follow a truncated power law according to

$$p_{on}(t_{on}) = p_0 t_{on}^{-\alpha_{on}} e^{-\Gamma_{on} t_{on}} \quad (2)$$

with $\alpha_{on} = 1.63$ and $\Gamma_{on} = 5.84\ s^{-1}$.

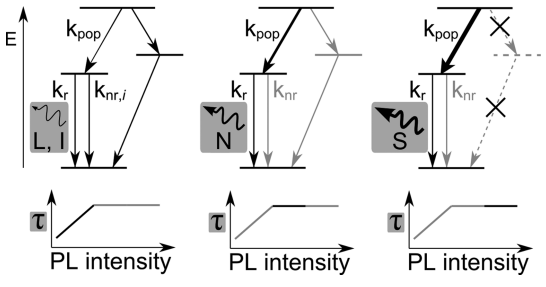

Figure 4. Population dynamics and PL intensity-dependent lifetime in a core/shell QD. PL intensities L, I, N, and S (see text) are shown as a function of hot electron relaxation. Spikes S are observed in the case that the nonradiative bypass is blocked (see text).

To be more specific, we investigate the on-time distribution with respect to each intensity level separately *via* CPA. To proceed, we collect all intensity-resolved on-time durations within the total PL time trace (15 min) and determine respective on-time distributions for each intensity level. The resulting on-time distributions are fitted by exponential decay functions leading to time constants, which we termed "τ_{macro}" (in analogy to "τ_{micro}" gained from PL decays curves). The fitted times are sorted with respect to the respective PL intensity. In the given example the decay curves of each clustered intensity level can be fitted (within 5%) by a monoexponential function. Figure 2b shows on the macrotime scale a typical intensity-dependent τ_{macro} distribution. At intensities corresponding to the noise level (<2 kcps), the dependence follows a power law as expected. Again, we first postpone the discussion of intensities S. The intensity-dependent distribution of τ_{macro} of the respective intensity levels (L to N) is in the range of (10−120) ms (Figure 2b). τ_{macro} is long ((35, 120) ms) for N and L intensities, respectively, but shorter ((10−15) ms) in the range I. For some QDs with a very high *QY* and in the presence of a high density of intensities in the N range (see Figure 1d), we find a biexponential decay with a second time in the range of (20−100) or (5−20) ms depending on the matrix. Details of this are described in the Supporting Information.

For the spike intensity S we observe a very fast (≈ 1 ms) monoexponential decay (Figure 2b). For CdSe/ZnS in the polar matrix PVA decays are shortened by about a factor of 2−4 (see Supporting Information) but behave qualitatively the same as for PS. This is in satisfying agreement with recently reported data for on-times in different dielectric environments.[14]

In the following we will discuss times τ_{macro} in more detail. One of the advantages of CPA is the possibility to relate on-time dynamics not only to a well-defined PL intensity but also to monitor the dynamics of intensity jumps ΔI between different intensities I. Keeping in mind that each intensity level is related to only a small number of electronic states, this offers the possibility to address dynamic properties in and between these states very specifically. For a QD of the type shown in Figure 2 (QD9 in PS, nondense N intensities) Figure 5a reveals that most of the intensity jumps ΔI from one arbitrary intensity to the next one are relatively small ($\Delta I = \pm 5$ kcps) as can be concluded from the half width of the intensity jump distribution. Neglecting both the smallest, probably noise-related intensity jumps, and the jumps from and to the intensity spikes S, we obtain typical jumps of $\Delta I = \pm 8$ kcps, while the largest jumps occur with $\Delta I = \pm 17$ kcps.

A further variable that can be directly related to the PL intensity is the, on the microtime scale measured, average PL lifetime τ_{micro}^{av} of a certain intensity level of index n_j before proceeding to a different intensity level

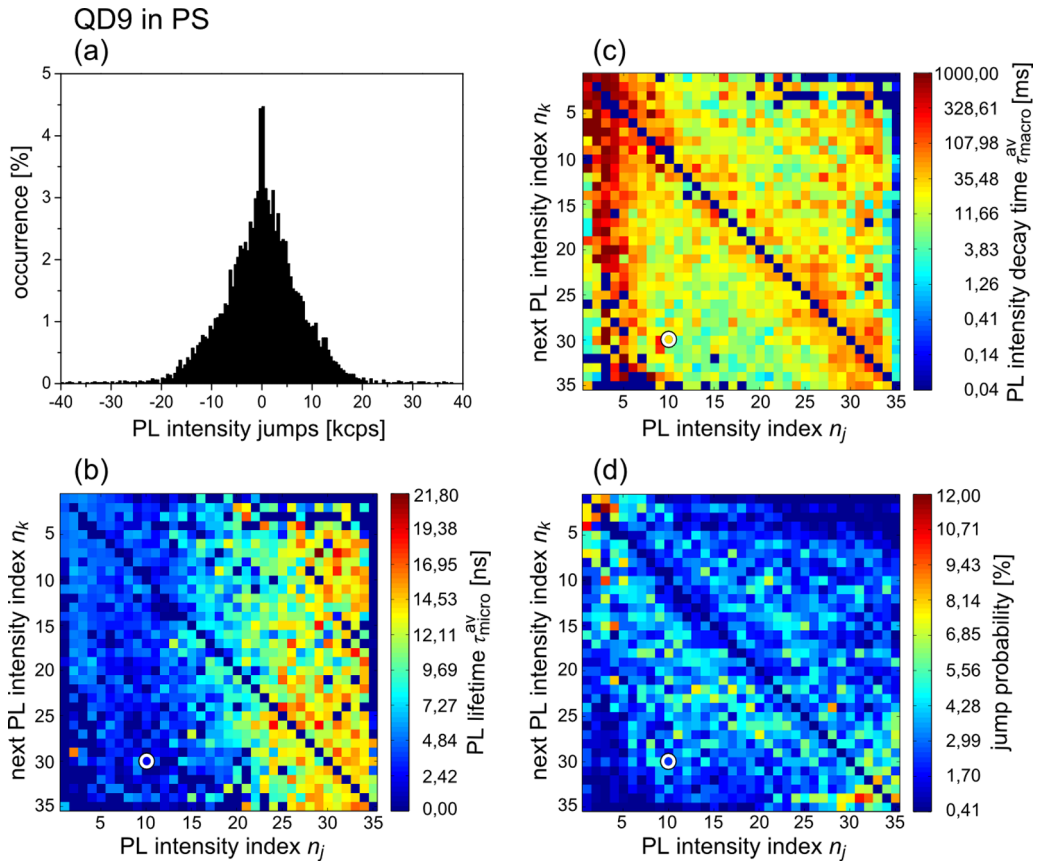

Figure 5. Jump dynamics of consecutive clustered PL intensity levels for the single CdSe/ZnS QD9 in PS from Figure 2. (a) Distribution of intensity jumps ΔI. (b) Algebraic averaged PL lifetimes τ^{av}_{micro} (color code) as a function of clustered intensities n_j before jumping to the next intensity n_k (c) Algebraic averaged intensity decay times τ^{av}_{macro} (color code) as a function of clustered intensity n_j before an intensity jump to the next intensity n_k. Note the long time of τ^{av}_{micro} for $n_j \approx 4$, independent of n_k. (d) Algebraic averaged jump probability (color code) for an intensity jump from intensity n_j to n_k. The same notations apply as for (c). The white circles in (b−d) relate to an example of how the graphs should be interpreted as a relation between the "starting" intensity level $n_j = 10$ jumping to $n_k = 30$. We have chosen a linear scale n_j, n_k for clustered intensities I since the distribution of spike intensities (S) is much less dense as compared to those for the other intensities.

n_k (Figure 5b; see Figure 2d for definition of the intensity level index n of this QD), during the complete time trace. Figure 5b shows that the nonexponential PL decay is not caused by the interrelation among different I_n and is therefore due to other reasons as will be discussed later. τ^{av}_{micro} is by definition different from τ_{micro} determined in the previous section since it equals the algebraic average of PL lifetimes determined in each case the intensity level jumps from n_j to n_k Not surprisingly, the data shown in Figure 5b are in close agreement with those presented in the quasi integrated form in Figure 2c (QD9 in PS in both cases). However, we now can additionally evaluate how the individual intensities $n_{j,k}$ are interrelated. No significant dependence of τ^{av}_{micro} is observed with respect to the next state index n_k. τ^{av}_{micro} decreases nearly monotonously with intensity from about 14 ns ($n = 28-34$) to 2−5 ns ($n = 3$). This is in general agreement with the fitting data shown in Figure 3, where we additionally observed an increasingly nonexponential decay with decreasing intensity. This is masked in the τ^{av}_{micro} representation because of formation of an algebraic average. Note, however, that τ^{av}_{micro} is slightly increasing for $n_j < 5$ in agreement with data for τ_{micro}.

Analogue to the PL lifetimes, we show the (algebraic) averaged on-times τ^{av}_{macro} for each intensity level n_j before entering the next level n_k in Figure 5c. This provides similar information as the one given in Figure 2b, but selected with respect to the next state. We also evaluate the probability to proceed from n_j to n_k (Figure 5d). Since we observed the reverse process ("backward", *i.e.*, jump from the previous intensity level instead of jump to the next intensity level) to be in all cases very similar to the "forward" one shown here, we will not discuss the latter separately.

We will now describe in more detail the relation of τ^{av}_{macro} on PL intensities. Times τ^{av}_{macro} (n_j, n_k) are in most cases independent of n_k. Though τ^{av}_{macro} is by definition different from τ_{macro} shown in Figure 2b, a comparison reveals many similarities, namely, 4 intensity related on-time regimes (see Figure 2d for definitions of intensity ranges): (i) a broad distribution (see color code) of τ^{av}_{macro} for $n < 3$ (noise background), (ii) a relatively long $\tau^{av}_{macro} > 100$ ms for $n \approx (3-5)$ (range L),

(iii) a nearly continuously increasing $\tau^{av}_{macro} \approx (10-30)$ ms for $5 < n \leq 33$ (range I and N), and (iv) a very short $\tau^{av}_{macro} \approx (0.5-1)$ ms for $n > 33$ (intensities S).

Two observations immediately emerge from Figure 5c. First, the lowest intensities ($n < 3$) correspond to background (BG) noise and are therefore broadly distributed in time. Second, the identification for a relatively long τ^{av}_{macro} for $3 < n < 5$ is a very strong indication of the presence of a specific PL intensity level (within the L regime) somewhat above BG. We like to point out that we observe the same phenomenon for all investigated QDs, which means that we can identify a very low PL intensity above BG, which might have been previously overlooked as has been also found recently.[10,20,41]

The jump probability in Figure 5d shows several distinct features. At the "end points" of the indicated "diagonal" (transition probabilities among predominantly small or predominantly large n, respectively) we observe a relatively high jump probability (see color code). This implies that jumps among very high (low) intensities N−S (BG−L) are more likely than those to other intensities. This observation is not masked by noise fluctuations, since in that case we would expect the same behavior along the diagonal, which is obviously not the case.

Other features differ systematically among different types of QDs.[39] However, in case that a truncated power law applies very large intensity jumps (*e.g.*, between $n = 3 \leftrightarrow n = 32$), are very unlikely (blue colored areas at the ends of the secondary diagonal), while they become more probable[39] in case of a deviation from a truncated power law. Additionally, jumps from and to $n = 35$ (intensity S) are restricted almost to N intensities. A general observation is that intermediate and small intensity jumps dominate. All this is in accordance with the jump distribution shown in Figure 5a.

Figure 6b shows the fluctuations of the PL emission energy of the single QD7 on SiO_x as a function of clustered PL intensity. It can be clearly seen that there is a considerable fluctuation (spectral diffusion) of PL energies for each intensity, which is larger than the noise-related fluctuations. However, on average low intensities are observed more likely at low energies, whereas high intensities correspond to high energies as indicated by the diamonds in the graph. The overall energy distribution amounts to about $\Delta E > 60$ meV.

Interrelation of Micro- and Macrotime Scales. To compare on-time and PL lifetime dynamics, we have in principle to refer to 2 different classes A and B of the investigated QDs as characterized by the overall distribution of intensities. Class A QDs show a homogeneous intensity distribution in the intensity range I to N (see Figure 2d). They can be described for each intensity I_n by a distribution of a varying but nearly monoexponential τ_{macro} over the total intensity range L to S, but contrary and unexpectedly by a biexponential PL decay (with

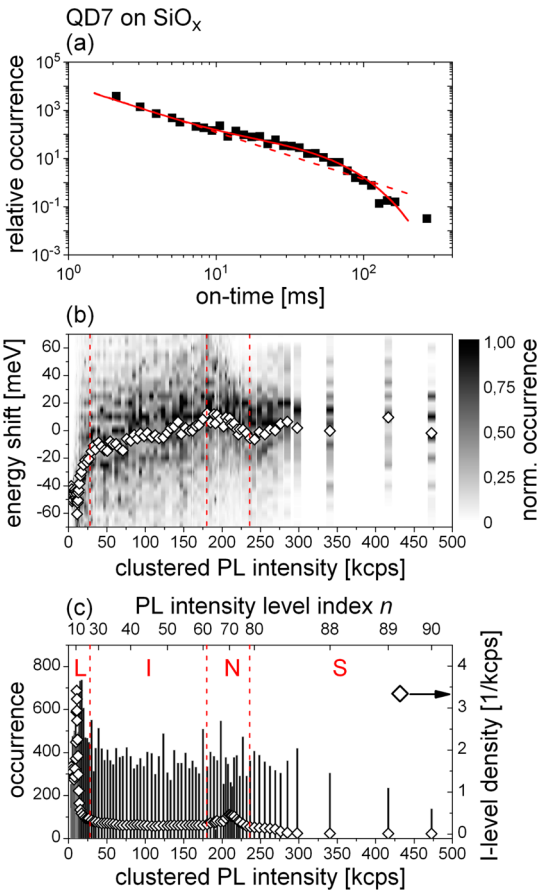

Figure 6. (a) Conventional (binned) on-time histogram of the single CdSe/ZnS QD7 on SiO_x. The red solid line indicates a fit according to a superposition of a truncated power law and an additional exponential decay according to eq S1 in the Supporting Information,[14] whereas the dashed line depicts a power law without truncation for comparison. (b) Distributions (see gray scale on the right) of spectral positions of PL energies as a function of PL intensity. Diamonds correspond to the average PL energy. Spectral positions are given by means of energy shifts ΔE with respect to the splitting wavelength of a dichroic beam splitter (predefined to $\Delta E = 0$ meV, see the Supporting Information) at $\lambda \approx 565$ nm (2.2 eV). Note that in the intensity range L, the real spectral position of the related short component $\tau_{micro,3}$ (Figure 3) is superimposed by the other two components $\tau_{micro,1}$ and $\tau_{micro,2}$ (see text for explanation). (c) Corresponding distribution of clustered PL intensities and related density (diamonds). Intensity ranges L, I, N, S as well as intensity level index n are also given. The dense N intensities relate to the deviation from the truncated power law in (a).[37]

lifetimes $\tau_{micro,1}$ and $\tau_{micro,2}$) in the L and I range. At very low intensities L (but clearly above the noise level) we find a narrow intensity range with a third very short PL decay component $\tau_{micro,3}$ accompanied by an increased density of intensities. These QDs exhibit in a threshold based analysis a truncated power law contrary to those of class B (see Figure 1c).

Class B QDs will be discussed in the Supporting Information in more detail. They show similar features as class A but with the exception that we find an increased density of intensities in the N-range (Figure 1d) accompanied by a slight increase of τ_{micro} from 14 to 15 ns in that range (Figure 1e) and a

biexponential distribution of on-times $\tau_{macro,i}$ in the range of high densities of intensities with $\tau_{macro,2} \approx 4\,\tau_{macro,1}$ (see Supporting Information). In general, class B QDs are different from class A ones in that they obviously are characterized by an additional well-defined state, which, *e.g.*, might be related to the presence of OH-groups.[16] On PVA, we only observe class B type QDs.[39]

DISCUSSION

Before we start a detailed discussion of PL intensity-dependent on-times τ_{macro} and PL lifetimes τ_{micro}, we will summarize a few essential facts that are inherent for blinking and PL decay phenomena in QDs. It is well-known that the PL decay of single QDs is non-exponential in the ns regime with exception at the highest PL intensities.[35−38] Several investigations explicitly relate the nonexponential PL decay to the PL intermittency.[10,35,36] Cordonnes *et al.*[20] and Galland *et al.*[41] found fluctuating PL decay times for low PL intensities during one and the same on-time period. From this they conclude that the long-time charging model does not hold.

Blinking reveals a broad distribution of on- and off-times as has been analyzed by threshold-based approaches. The off-times are in most cases described by a power law with an exponential cutoff at long times.[2−6,14] Both the power law exponents and the cutoff times depend on the embedding environment,[14−16,39] the core−shell interface,[42] the crystal morphology, and the type of ligands.[43]

Besides the evidence of a power law and an exponential cutoff for on-times, a superimposed additive exponential term has recently been reported and related to specific (hole) traps.[16] Moreover, on-time distributions depend on excitation wavelength,[40] excitation power,[44,45] temperature,[46] and the QD interface.[47] Recently we reported[14] that the exponential cutoff of on-times depends strongly on the dielectric constant of the embedding matrix as off-times do,[15] while the superimposed exponential contribution depends, for example, on the concentration of surface[16] or matrix OH-groups.[39]

An explicit goal of the present blinking analysis *via* CPA is to get rid of the implications of a threshold-based analysis. In Figure 2a,b we compare the distribution of on-times as determined by the conventional threshold procedure with CPA-based results for a typical single CdSe/ZnS QD in PS, respectively. The threshold-based on-time statistics show a truncated power law according to eq 2 with a truncation time of $\Gamma^{-1} \approx 170$ ms and an apparent deviation from an exclusive power law at $t_{on} \approx 35$ ms, respectively. These times are in agreement with those for the same QD identified by CPA up to $\tau_{macro} \approx 120$ ms and $\tau_{macro} \approx 35$ ms as determined for intensities L and N, respectively. However, while CPA data collect the exponential decay

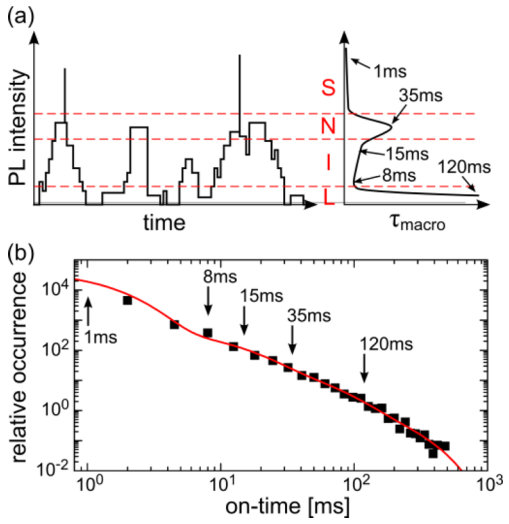

Figure 7. (a) Schematic presentation of the time dependent PL intensity (left) and the corresponding decay times τ_{macro} as a function of clustered intensities *I* (right). (b) Fit of the on-time histogram (see Figure 2a) by five exponential decay functions with fixed decay times $\tau_{macro,i} = \{1, 8, 15, 35, 120\}$ ms (see (a) and Figure 2b) instead of a truncated power law.

of each PL intensity separately, threshold-based data sum-up all on-times for all PL intensities. Inspection of CPA reveals (only) a few S intensities, which decay within less than 1 ms. Intensities L, I, and N decay with times between $\tau_{macro} \approx 10$ ms and $\tau_{macro} \approx 120$ ms. Thus, the overall distribution of exponential times τ_{macro} is about 1 order of magnitude (neglecting the intensities S). We conclude that the apparent power law-distribution stems from a superposition of a distribution of (intensity-dependent) exponential functions. A schematic presentation of our findings is shown in Figure 7 together with a 5-fold exponential fit of the threshold-based apparent power law (compare Figure 2a) characterized by $\tau_{macro,i} = \{1, 8, 15, 35, 120\}$ ms. Very importantly, on-times determined by CPA are extremely sensitive to the embedding matrix as shown in the Supporting Information and are shortened at all intensity levels by about a factor of 3 to 4 when changing from PS (with a dielectric constant $\varepsilon = 2.5$) to PVA ($\varepsilon = 14.0$). This is in qualitative agreement with results for power low-truncation times Γ^{-1} as obtained from threshold-based analysis.[14]

The CPA-based analysis demonstrates that a power law behavior is only a rough approximation and that a much narrower distribution of "switching" times is sufficient to cover the experimental results. This corroborates the recently suggested model of multiple recombination centers,[23] which identifies less than 10 traps to be responsible for blinking processes in various quantum systems. At this point we arrive at the important conclusion that the power law-type distribution of on-times stems from a superposition of intensity-dependent but well-defined "switching processes", the time scale of which is controlled by the concrete properties of the QD and its environment.

The involvement of charges or a polar character of the switching rates is supported by the strong dependence of on-times (and off-times)[15] on matrix polarity.

As can be seen in Figure 5a, intensity jumps are symmetrically distributed with respect to a decrease or increase of intensity. Most of the intensity jumps related to the (8−120) ms on-time regime are small (corresponding to small changes in the electronic properties). This implies that in this type of QD a complete on−off (or off−on) process is realized in several small intensity steps. Only processes related to the very short (<1 ms) on-time regime occur predominately in one step (namely, between intensities S and N and vice versa). These findings are a strong indication that relatively few PL quenching processes (some of them are even well-defined[16,39]) are active as has been also found recently.[23,31] This is also supported by experiments on an analogous CdSe/ZnS QD, which exhibit t_{on} = 40 ms.[10]

After having reinterpreted the statistics of on-processes with respect to a power law type behavior, we attempt to set up a mechanistic model to explain the underlying physical background. As a starting working hypothesis, we suggest that each PL intensity corresponds to one or a set of very few well-defined electronic QD states. The PL intensities of these states will be controlled by nonradiative quenching rates. Whether such a quenching applies relies on the coupling to relaxation (recombination) centers which will be switched on and off as characterized by a switching rate. In fact, such a switching corresponds to the presence of 2-level systems as has also been suggested recently[23] and is closely related to the postulated disorder to be a prerequisite for blinking.[2] In case PL intensities can be identified with closely related electronic states, this idea should be also transferable to the intensity jumps. While a small jump in PL intensity will be related to an only small change in the overall electronic configuration, a large intensity jump will be identified with a considerable one or a drastic change in the population probability.

Unique spectroscopic signatures of a specific electronic state are PL energies and PL lifetimes. PL energies have been found to fluctuate by less than 25 meV during a whole sequence of blinking events excluding for the moment intensity range L (see Figure 6b). This indicates that independent of the large variation of PL intensities, differences of the electronic configuration must be small. PL lifetimes, however, vary considerably. According to this one would at first glance expect that CPA of PL intensities would allow to assign each intensity to exactly one PL lifetime (τ_{micro}) as has been found for the on-times in the macrotime regime. However, the situation is far from being that simple, since obviously CPA-based PL lifetime evaluation (see Figure 3) reveals 2−3 decay times in the intensity range L and I but only 1 in the range N and S. It is a most remarkable feature that the PL lifetimes depend only weakly on the embedding matrix (a typical comparison for PS and PVA is shown in the Supporting Information), which is in contrast to the on-time behavior. We take this as a strong indication that τ_{micro} reflects basically intrinsic electronic properties of the core/shell system.

We will discuss the two intensity ranges (L, I) and (N, S) separately and start with the former. We clearly observe a deviation from a monoexponential PL decay in this intensity range. This implies that for one selected PL intensity I, at least two distinguishable electronic states have to be assigned differing in the decay rate $1/\tau_{micro} = k_r + k_{nr}$ and in rates $k_{nr,i}$ (while assuming similar rates $k_{r,i}$) since they would not show the same PL intensity otherwise (see eq 1 and following annotations). Since we relate intensities with electronic states, the presence of different states in close energetic proximity at the excitonic band edge is in agreement with recent experimental findings.[30−32,47] According to calculations[48,49] energies and dynamics of band edge states depend on surface, interface, ligands, and charging conditions. Jones *et al.*[31] have shown that distributions of trap state energies result in a (temperature-dependent) multiexponential PL decay of QD ensembles. Instead of the presence of traps, an alternative explanation is the formation of charged QDs (trions) where the charge is in the core or on the shell of the QD.[17] The presence of such states will be accompanied by internal Stark effects. We suggest that both explanations might apply,[24] and that "softening" of the band edge in addition to charging processes is the physical background of the (nonexponential) PL decay observed even for well identified intensities.

Additionally, some publications consider bi- or even multiexcitons to be involved in PL dynamics of QDs and to be (at least partly) responsible for blinking.[50] In this case also, Auger processes emerge, leading to nonradiative recombination pathways. To estimate the influence of multiexcitons in this study, we calculate the number $\langle N \rangle$ of absorbed photons per excitation pulse.[44] With an absorption cross section of about $\sigma \approx 1.5 \times 10^{-15}$ cm^2 at the used excitation wavelength (465 nm), this gives approximately $\langle N \rangle \approx 0.1$ and a still lower probability for biexciton generation. Though biexcitons will probably be formed on time scales of blinking experiments one has to take into account very low ionization probabilities finally resulting in PL suppression.[44] Furthermore, we also investigated CdSe/CdS QDs with a larger core diameter (PL emission maximum at about 610 nm) and 5 to 6 monolayers of CdS. For this QD the related absorption cross section of $\sigma \approx 10^{-14}$ cm^2 is about 1 order of magnitude higher and gives $\langle N \rangle \approx 0.75$. Nevertheless all optical properties evaluated by CPA show nearly the same results as we have found for CdSe/ZnS QDs. From this we concluded that the influence of multiexcitons is negligible at least in the present case.

How can we explain the strongly intensity-dependent PL lifetimes $\tau_{micro,1}$ and $\tau_{micro,2}$? The nearly linear relation of both times with PL intensity supports the variation of the *QY* according to eq 1, which reflects the fact that electronically similar states are quenched nonradiatively by coupling to (a distribution of) relaxation centers. The time scale for switching between different relaxation channels is given by the on-time distribution (see Figures 2b and 7). Obviously both tentatively assigned electronic states have a characteristic intrinsic lifetime differing by about a factor of 3 at the respective highest intensity. Consequently, assuming similar radiative rates, the nonradiative rates also differ by *at least* a factor of 3 (depending on the absolute value of radiative rates). However, the state related to $\tau_{micro,2}$ contributes significantly more in the range of low intensities L but not in the range N. From this we conclude that this state is more sensitive to nonradiative relaxation processes than state 1, which probably decays at the highest intensity predominantly radiatively. Furthermore, the population rate of state 2 must be higher with respect to state 1 to enable different PL lifetimes $\tau_{micro,i}$ for identical PL intensities in case of similar radiative rates (see eq 1).

As we have shown in Figure 3a the contribution of a short lifetime $\tau_{micro,3}$ <1 ns is only observed in a narrow intensity range at very low PL intensities L. Recently Galland,[41] Cordonnes,[20] and Amecke[10] identified very low intensity levels, for which they conclude that they are due to charged (hole in the QD core) QDs, which show a remaining PL since Auger effects in combination with ionization probabilities are not strong enough for a complete quenching. Further on in the discussion we will suggest an alternative explanation.

Now we turn to the intensity range (N, S) in which the intensities change but the lifetime remains constant as can be seen in Figure 3. Following eq 1, this is not in agreement with the *QY*-model, but can be explained, as already mentioned, by formation of hot charge carries in combination with a variation of population pathways (schematically shown in Figure 4). Independent of the population rate, we will always observe the same PL lifetime τ_{micro}. CPA analysis shows that the related τ_{macro} distribution in this intensity range is between 35 ms and less than 1 ms. Effective blocking of the alternative nonradiative decay route (as visible by the appearance of spikes S) is obviously a short event with times shorter than 1 ms (PS) or even shorter than 0.2 ms (PVA).

Finally, we to set up a generalized model presented in Figure 8 taking into account up to 3 different emissive electronic states, which are at least in part trap states. This assumption is reasonable since we identified 3 decay times in the intermediate (I) and low (L) PL intensity range. This model explains at least most of our findings.

The basic ideas of our model are that after excitation the hot electron−hole pair relaxes partly (for the additionally involved nonradiative bypass of hot electrons/holes, see Figure 4) to the respective band edges. From there, both the ground state or a manifold of trap states can be populated, which themselves decay *via* radiative or (variable) nonradiative routes to the ground state. In a certain sense this model resembles the one of Knowles *et al.*[33] for time-resolved PL decay investigations on an ensemble of QDs. In case of single particle blinking the various relaxation pathways are not available in parallel within one excitation cycle, but the QD decay is routed *via* gates to various relaxation channels. Exactly this gating results in blinking on time scales between about 8 and 120 ms. What has to be discussed in the following is the minimum number of traps and gates to be taken into account in order to describe the experimental findings in general.

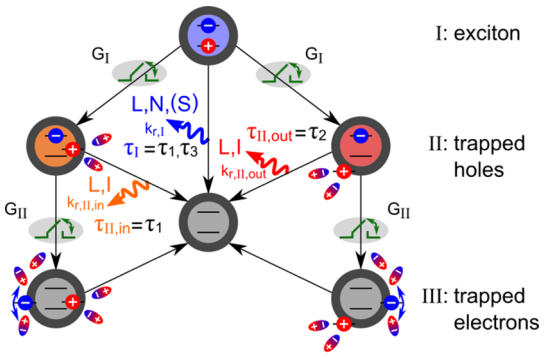

Figure 8. Schematic population and switching dynamics in a core/shell QD: hierarchy of exciton (I) relaxation *via* hole (II) and electron trapping (III). Wavy lines denote the three radiative transitions with corresponding PL intensity ranges (L, I, N, S), wavelength of the PL (see colors of lines, QDs and letters), and PL decay times (τ_I, $\tau_{II,in}$, $\tau_{II,out}$; indices in and out indicate trap position of the hole within the QD shell), related with experimental PL lifetimes (τ_1, τ_2, τ_3; τ stands for τ_{micro}). We assume similar radiative rates $k_{r,I} \gtrsim k_{r,II,in} \gtrsim k_{r,II,out}$. Gate symbols denoted by G_I and G_{II} switch decay channels accessible (gate open) or blocked (gate closed, see also Figure 9). In case of open (closed) gates G_I the decay of the exciton (I) is characterized by a low PL intensity L (N) and a short (long) PL lifetime τ_3 (τ_1). We assume only 2 hole trapping configurations visualized by trapping at the inner (left side, index in) or outer shell interface (right side, index out). Electron trapping is assumed to follow a broad distribution of processes indicated by the double arrow among schematic electric dipoles.

First, what type of "traps" have to be considered? It is evident that the majority of traps are of common nature since a very similar intermittency behavior is observed for all types of colloidal QDs.[2−6,23] Two main sources for traps immediately emerge, namely, hole and electron traps, which are formed in the band gap, for example, because of unsaturated dangling bonds of Cd and/or Se atoms, respectively. Recently Frantsuzov *et al.*[23] proposed a model of multiple recombination centers assuming trapping of holes. Calculations show[48,49,51] that the properties of such traps depend specifically on crystal structure, capping layer, ligands, environment, and electric dipole moments of the respective QD. Alternatively, Kern *et al.* propose[34] that

electron traps are the origin of blinking processes of single QDs. It has been concluded that a combination of hole and electron trapping is needed to explain the on-times and the nonexponentiality of both PL decays (of bulk and single QDs).[12,14,16,33] An alternative concept to explain the properties of trap states relies on the presence of structural and electronic asymmetries created at the QD surface/interface and is based on mixing of electronic states within the fine structure manifold of QDs.[32] Relating our present findings with those of already reported results, we suggested that QDs are subject to the influence of both electron and hole trap states. In our approach we suggest that the two identified times $\tau_{micro,1}$ and $\tau_{micro,2}$ characterize two different radiative (classes of) traps, which we tentatively assign to trapped holes (*e.g.*, at the inner and outer interface of the ZnS shell, see Figure 8). Both kinds of trapped holes are allowed to couple to a manifold of electron traps, which results in shortening of the respective hole trap lifetimes $\tau_{micro,i}$.

To simplify the further discussion and the necessary introduction of gates, we refer to the suggestive scheme shown in Figure 8 and explain it step by step. According to Figure 6b, PL intensities in the intensity range N belong to the energetically highest states shifted on average to the blue by at most 25 meV relative to those in the I and S range. Additionally, we find by a combination of time-resolved and spectral analysis that the PL related to the short-lived component $\tau_{micro,3}$ in intensity range L also occurs predominantly in the blue PL range (see Supporting Information). (Note in this context that for such low intensities, the real spectral position of $\tau_{micro,3}$ is superimposed by the other two components $\tau_{micro,1}$ and $\tau_{micro,2}$ despite their small relative amplitudes (see Figure 3) because of their much longer decay times, resulting in a larger number of photons emitted from these components compared to the fastest one.) We suggest that in a first step the thermally relaxed exciton (hierarchy I, top of Figure 8) decays either radiatively (blue wavy line for radiative rate $k_{r,I}$) upon electron–hole recombination or, predominantly, nonradiatively by hole trapping ($\tau_I = \tau_{micro,3}$, intensity range L). We do not state that this exciton is the originally formed one, but it might be a relaxed one as several optical transient experiments suggest.[33,52]

The nonradiative channels populate at least 2 redshifted hole-trap states (hierarchy II, hole traps at, *e.g.*, inner (index in) or outer (index out) shell interface). We need at least 2 distinguishable trapped hole states since we observe in the (L, I) range 2 PL decay times $\tau_{micro,1}$ and $\tau_{micro,2}$. It is reasonably to assume that these hole traps are well characterized as has been shown by recent calculations.[51] We find a relatively slow switching process (indicated by "gates" G_I in Figures 8 and 9), which blocks and opens these nonradiative channels between hierarchy I and II on time scales of ≈ 120 ms (L → I, N) and ≈ 35 ms (N → I, L) as can be deduced from

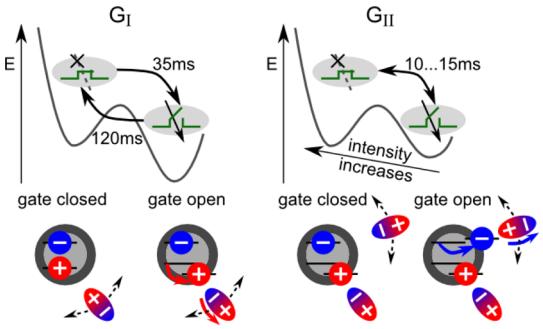

Figure 9. Two-level gates G_I (between hierarchies I and II, see Figure 8) and G_{II} (between hierarchies II and III) and corresponding switching times. In case of closed (open) gates the respective trap states for holes or electrons are blocked (accessible) because of a corresponding orientation of dipoles nearby the outer interface of the QDs.

Figures 5 and 7. In case of open gates G_I the decay of the exciton is characterized by a low PL intensity (range L) and a short PL lifetime $\tau_I = \tau_{micro,3}$ due to effective nonradiative hole trapping pathways. Vice versa, closed gates G_I strongly reduce the overall nonradiative rate (the nonradiative contribution to electron–hole recombination still remains) leading to PL intensities in range N and a long PL lifetime $\tau_I = \tau_{micro,1}$. The trapped holes can recombine radiatively with the electrons with similar radiative rates ($k_{r,I} \gtrsim k_{r,II,in} \gtrsim k_{r,II,out}$) but strongly different nonradiative rates accounting for the different decay times $\tau_{II,in} = \tau_{micro,1}$ and $\tau_{II,out} = \tau_{micro,2}$, whereas the PL intensity is the same due to variable population rates (see above).

Finally (on hierarchy III), also the electron will be trapped occasionally. Now electron and hole can no longer radiatively recombine as typical for deep (intraband) trap states. The existence of deep, weakly emitting intraband states has been reported, for example, by Knowles *et al.*[33] Since the wave function of an electron is more extended in space than that of a hole, a large variety of such trapped electrons can be realized.[53] Additionally, trapped electron states will be very sensitive to the embedding environment.[2,14−16,26,39]

In a next step we have to discuss the dynamics among the three hierarchies I, II, and III, respectively, which will constitute the PL intermittency scheme. Though CPA revealed more than 40 clustered intensities, at most 6 basic electronic states (including the ground state) are sufficient to describe the PL decay. Additionally, the absolute number of clustered intensities will depend on the clustering algorithm. Further on, besides in the low and high PL intensity range (typically assigned as off- and on-states, respectively), intensities are nearly homogeneously distributed.

How can this apparent contradiction of 40 and more clustered intensities but only 6 electronic states be solved? Obviously the time scale of apparent on-times (see Figures 2b and 7) is quite narrow (opposite to what is expected from a power law) and can, in the given

example, be roughly characterized by the 4 times 120, (8−15), 35, and 1 ms, respectively. The latter belongs to the PL intensity range S and has been assigned to variations in the population route as shown in Figure 4. We therefore conclude that switching dynamics are much less heterogeneous than intensities are. According to this conclusion we assume that that nonradiative rates between hole trap states (hierarchy II) and electron−hole trap states (hierarchy III) vary strongly, depending on the conditions of (matrix-influenced) electron trapping.

The simplified overall dynamics among the three hierarchies can be followed in Figure 8. The channels to proceed from I to II and II to III are not open all the time, but are switched "unblocked" or "blocked" on a slow time scale (macrotimes τ_{macro}). This is indicated schematically in Figure 8 by gates G_I and G_{II}. Such gates correspond to a coupling of the excited state to a two-level system (Figure 9).[23] Herby we assume that we are not sensitive enough to discriminate between the routes between the 2 different types of hole traps. According to Figure 2b, τ_{macro} for intensity range N is close to 35 ms. But what is the microscopic trapping rate for the crossover from I to II? We propose that the decay time $\tau_{micro,3} \approx 1$ ns can be identified with this rate since this time has been identified in a rather narrow intensity range (see Figures 3b and 5b). In case that this assignment is correct, a further conclusion immediately emerges from this identification. For the lowest PL intensities, we observe $\tau_{macro} \approx 120$ ms. Following the previous argument this implies that the gate between I and II is not "symmetric". It opens (channels get unblocked: N → I, L) within $\tau_{macro} \approx$ 35 ms and closes (channels get blocked: L → N) within $\tau_{macro} \approx 120$ ms (see Figure 9).

While the gate acting on the exciton (hierarchy I) reveals basically only 2 switching times, the 2 hole-trap states (of hierarchy II) show, as we have already outlined, a broader distribution of PL intensities and PL lifetimes τ_{micro} but a narrow distribution of switching times $\tau_{macro} \approx$ (8−15) ms. The origin of this finding is that, within the suggested model, the nonradiative trapping rates between hierarchy II and III depend on a manifold of accessible electron trapping configurations, which causes a considerable variation of the transition rates between II and III. According to eq 1 and the related discussion, the trapping rates will determine the PL intensities (of the hole traps) over a broad continuously distributed range. On the contrary, the switching times in this range vary much less, indicating the presence of basically only one gating process. In Figure 9 we propose an elementary process for such gates, which is the flipping of an electronic dipole at (various) positions at the outer interface of the QD, simultaneously allowing for the observed coupling to the dielectric properties of the environment and/or surface states.

According to the model given in Figure 8, the PL intermittency is rather the consequence of switching nonradiative trapping rates on and off than of a long-time charge trapping. Our experiments are a direct proof of the related conjectures suggested recently.[23,24] Moreover, the related analysis of macrotimes clearly reveals that the apparent power law behavior previously attributed to on-times is in fact a convolution of a few τ_{macro} (which will additionally depend on the threshold and binning time[28]). Referring again to the MRC model,[23] we can roughly identify 4 switching times τ_{macro} for the given example, namely, $\tau_{macro,1} \approx 1$ ms (population pathway), $\tau_{macro,2} \approx 35$ ms (switching N off), $\tau_{macro,3} \approx 120$ ms (switching L off), and $\tau_{macro,4} \approx$ (8−15) ms (switching I on or off). The number 4 is very close to the one proposed by Frantsuzov *et al.*[23]

We have suggested two different (radiative) hole trap states, which is certainly somewhat arbitrary. However, this approach is prompted by the observation of at least 2 PL decay times for one and the same PL intensity. In many ensemble experiments the non-exponential decay can be satisfactorily fitted by three decay times, one in the range of the "normal" PL lifetime, a shorter second one about at half of this time, and a third one in the range of 1 ns.[30−34] Additionally, though we have discussed basically our findings for only one single QD for clarity, the results for all together 60 QDs are qualitatively similar though absolute values may vary. More examples are given in the Supporting Information.

Finally we like to add a few comments on the origin of τ_{macro}. Since the switching times depend on the matrix and specific interactions[39] they are not an intrinsic property of the QD core, but of the (inner and outer) interfaces. We have observed a clear dependence of these switching times (and their distribution) on the polarity of the matrix.[2,14−16,39] Both on- and off-times become systematically shorter with increasing dielectric constant. We suggest that relatively slow local fluctuations of dielectric properties at the interface strongly influence the switching times of the trapping channels of holes and/or electrons, respectively. These fluctuations may be also influenced by local ligand dynamics since ligand binding takes place predominantly *via* electrostatic interactions.[54] Frantsuzov *et al.*[23] have suggested that displacements of surface atoms might give rise to the switching processes, which is an alternative or parallel trapping route supported by calculations of the mobility of surface atoms[55] and ligands and structure-related hole traps.[51]

CONCLUSIONS

CPA reveals that a threshold-free PL intensity analysis of QD blinking favors a hierarchical energy relaxation scheme as shown in Figure 8. The presented model relies basically on a trapping model assigning the short-lived intensity at a low PL intensity to the quenched exciton emission. Recent calculations have shown[48,49,53] that the energies and transition probabilities of band edge states (traps) of QDs depend

critically on the electronic properties of the surface (formation of surface trap states). This results in complex (multiexponential) PL decay dynamics on the microtime scale. In a (simplified) model we consider three classes of states, namely, (i) exciton states, (ii) (red-shifted) radiative hole traps, and (iii) nonradiative electron traps. The PL lifetime of the exciton state will be effectively shortened by a (switchable) nonradiative trapping to radiative band edge hole trap states. Switching among all these states (multiple trapping) occurs on long time scales with a limited number of about 4 different τ_{macro} in a range of typically (1−100) ms, which points to a few well-defined microscopic switching processes close to or at the QD interfaces.

We draw the important conclusion that on-times are not power law distributed, but have to be described by a superposition of a few switching processes, which corroborates the limited number of traps suggested by the multiple recombination center model.[23] Besides N ↔ S jumps, which correspond to large intensity jumps, intensity variations occur predominantly in small steps in case that dim or gray states are involved. Such intermediate intensities will only be observed in case of heterogeneous interfaces. Besides a broad distribution of PL intensities there are a few additional well-defined trapping states related to large intensity jumps. Though a power law is merely a convenient approximation, possibly without a strong physical background, several experimental observations conducted in terms of power-law models are nevertheless in qualitative agreement with those of the change point analysis.

In all cases for which blinking has been observed, strong disorder is present both in space and energy.[2] Such amorphous (glass-like) environments can be represented by a distribution of two-level systems. To the best of our knowledge, up to now no pronounced temperature dependence has been found.[2−6] This points toward tunnelling processes in a landscape of two-level systems involving the matrix, ligands, and surface reconstructions of the QDs interfaces.

METHODS

We used CdSe/ZnS QDs capped with trioctylphosphine oxide (TOPO) ligands. QDs were supplied by Invitrogen, Molecular Probes, now Life Technologies (Qdot 565 ITK organic quantum dots), with PL emission centered at 565 nm (fwhm 33 nm) and embedded in polystyrene (PS) films of about 20 nm thickness on silicon oxide by spin coating. We also performed experiments on CdSe/ZnS QDs spin coated onto a polyvenylalcohol (PVA) layer or a silicon oxide (SiO_x) substrate. Some of the investigated features depend critically on the matrix.[39] Details of the sample preparation and further results of more QDs are given in the Supporting Information.

To investigate QD blinking we used a home-built confocal laser microscope.[39] The QDs were excited by a 50 ps-pulsed laser diode (Picoquant, LDH-P-C-470) at 465 nm with an average excitation power of 500 nW at a repetition rate of 20 MHz focused through a high numerical aperture objective (Zeiss EC Epiplan Neofluar, 100×, NA 0.9). For each detected PL photon (avalanche photodiode, Picoquant MPD, PDM Series), the macrotime (relative to the beginning of the measurement, device inherent time resolution 50 ns, real time resolution, see below) and the microtime (relative to the laser pulse, time resolution 50 ps) were recorded leading to time-tagged and time-resolved (TTTR) single photon counting data.

These TTTR data were analyzed by the change-point analysis (CPA), developed by Watkins *et al.*[29] This method takes advantage of the Poisson statistics of photons, emitted by a single photon emitter, to identify constant PL intensities directly from a set of arrival times, photon by photon. The experimental resolution in the macrotime regime depends on the number of detected photons and results typically in 100 μs to 1 ms. Because no binning is needed, the occurrence of "false", binning related intermediate intensities is avoided. While CPA is able to detect states of constant PL intensity, the absolute intensity will depend on the number of emitted photons. This leads to continuously distributed PL intensities. To correlate these intensities with a finite number of PL intensity levels of the QD, a clustering algorithm, also developed by Watkins *et al.*,[29] is applied to the CPA data. As a result, all states of constant PL intensity with a similar distribution of photon arrival times are attributed to one of a finite number of intensity levels. Furthermore, for comparison with a threshold based method, the TTTR data were binned to obtain the common PL blinking time traces (binning time 1 ms). In general, the (theoretical) time resolution of CPA is predetermined by the given technical time resolution of the macrotimes (50 ns in our case). Nevertheless, the real time resolution depends on the current PL intensity of a certain QD due to an increasing statistical uncertainty with a decreasing number of detected photons. For example, intensities of about (20...40) kcps, which we typically measure in this study (intensity range N), lead to an average number of 10 detected photons within (250...500) μs; *i.e.*, the real time resolution is in the sub-ms range in this case. Therefore, CPA does not primarily result in an enhanced time resolution but, more important, in the (binning-free) determination of (real) intermediate intensity levels.

PL intensity time traces of single QDs were recorded for about 15 min by TTTR providing both macro- and microtimes. While the macrotime yields information on the elapsed time between two consecutive photons and thus the PL intensity (which equals simply the number of photons per time), the microtime allows the determination of the PL lifetime by creating a histogram over several photons related to the same PL intensity. Figure 1a shows a detail of a PL intensity time trace of CdSe/ZnS QD10 in PS obtained by binning (1 ms, black data) and reconstruction *via* CPA (red line). It is obvious that CPA represents on one hand the binned time trace and on the other hand is able to identify states of constant PL intensity. We also measured the PL spectra of the QDs as a function of PL intensity. Details of the related experimental set up and analysis are given in the Supporting Information.

Conflict of Interest: The authors declare no competing financial interest.

Acknowledgment. We acknowledge helpful discussions with Eduard Zenkevich (Minsk, Belarus).

Supporting Information Available: Further examples of single QDs with related macrotimes and microtimes in different matrices. Spectrally and intensity resolved PL decay of single QDs. Experimental details of sample preparation and fast determination of spectral position of QDs. This material is available free of charge *via* the Internet at http://pubs.acs.org.

REFERENCES AND NOTES

1. Nirmal, M.; Dabbousi, B. O.; Bawendi, M. G.; Macklin, J. J.; Trautman, J. K.; Harris, T. D.; Brus, L. E. Fluorescence Intermittency in Single Cadmium Selenide Nanocrystals. *Nature* **1996**, *383*, 802–804.
2. Cichos, F.; von Borczyskowski, C.; Orrit, M. Power-Law Intermittency of Single Emitters. *Curr. Opin. Colloid Interface Sci.* **2007**, *12*, 272–284.

3. Frantsuzov, P.; Kuno, M.; Janko, B.; Marcus, R. Universal Emission Intermittency in Quantum Dots, Nanorods and Nanowires. *Nat. Phys.* **2008**, *4*, 519–522.
4. Lee, S. F.; Osborne, M. A. Brightening, Blinking, Bluing and Bleaching in the Life of a Quantum Dot: Friend or Foe? *ChemPhysChem* **2009**, *10*, 2174–2191.
5. Ko, H. C.; Yuan, C.-T.; Tang, J. Probing and Controlling Fluorescence Blinking of Single Semiconductor Nanoparticles. *Nano Rev.* **2011**, *2*, 5895.
6. Riley, E. A.; Hess, C. M.; Reid, P. J. Photoluminescence Intermittency from Single Quantum Dots to Organic Molecules: Emerging Themes. *Int. J. Mol. Sci.* **2012**, *13*, 12487–12518.
7. Geddes, D.; Parfenov, A.; Gryczynski, I.; Lakowicz, J. R. Luminescent Blinking from Silver Nanostructures. *J. Phys. Chem. B* **2003**, *107*, 9989.
8. Bradac, C.; Gaebel, T.; Naidoo, N.; Sellars, M. J.; Twamley, J.; Brown, L. J.; Barnard, A. S.; Plakhotnik, T.; Zvyagin, A. V.; Rabeau, J. R. Observation and Control of Blinking Nitrogen-Vacancy Centres in Discrete Nanodiamonds. *Nat. Nanotechnol.* **2010**, *5*, 345–349.
9. Zhang, K.; Chang, H.; Fu, A.; Alivisatos, A. P.; Yang, H. Continuous Distribution of Emission States from Single CdSe/ZnS Quantum Dots. *Nano Lett.* **2010**, *6*, 843–847.
10. Amecke, N.; Cichos, F. Intermediate Intensity Levels During the Emission Intermittency of Single CdSe/ZnS Quantum Dots. *J. Lumin.* **2011**, *131*, 375–378.
11. Geller, M. R. Dynamics of Electrons in Graded Semiconductors. *Phys. Rev. Lett.* **1997**, *78*, 110–113.
12. Verberk, R.; van Oijen, A.; Orrit, M. Simple Model for the Power-Law Blinking of Single Semiconductor Nanocrystals. *Phys. Rev. B: Condens. Matter Mater. Phys.* **2002**, *66*, 233202.
13. Tang, J.; Marcus, R. Diffusion-Controlled Electron Transfer Processes and Power-Law Statistics of Fluorescence Intermittency of Nanoparticles. *Phys. Rev. Lett.* **2005**, *95*, 107401.
14. Issac, A.; Krasselt, C.; Cichos, F.; von Borczyskowski, C. Influence of the Dielectric Environment on the Photoluminescence Intermittency of CdSe Quantum Dots. *ChemPhysChem* **2012**, *13*, 3223–3230.
15. Issac, A.; von Borczyskowski, C.; Cichos, F. Correlation Between Photoluminescence Intermittency of CdSe Quantum Dots and Self-Trapped States in Dielectric Media. *Phys. Rev. B: Condens. Matter Mater. Phys.* **2005**, *71*, 161302.
16. Krasselt, C.; Schuster, J.; von Borczyskowski, C. Photoinduced Hole Trapping in Single Semiconductor Quantum Dots at Specific Sites at Silicon Oxide Interfaces. *Phys. Chem. Chem. Phys.* **2011**, *13*, 17084.
17. Jha, P. P.; Guyot-Sionnest, P. Trion Decay in Colloidal Quantum Dots. *ACS Nano* **2009**, *3*, 1011–1015.
18. Zhao, J.; Nair, G.; Fisher, B. R.; Bawendi, M. G. Challenge to the Charging Model of Semiconductor-Nanocrystal Fluorescence Intermittency from Off-State Quantum Yields and Multiexciton Blinking. *Phys. Rev. Lett.* **2010**, *104*, 157403.
19. Rosen, S.; Schwartz, O.; Oron, D. Transient Fluorescence of the Off State in Blinking CdSe/CdS/ZnS Semiconductor Nanocrystals Is Not Governed by Auger Recombination. *Phys. Rev. Lett.* **2010**, *104*, 157404.
20. Cordonnes, A. A.; Bixby, T. J.; Leon, S. R. Direct Measurement of Off-State Trapping Rate Fluctuations in Single Quantum Dot Fluorescence. *Nano Lett.* **2011**, *11*, 3366–3369.
21. Frantsuzov, P. A.; Volkán-Kacsó, S.; Janko, B. Model of Fluorescence Intermittency of Single Colloidal Semiconductor Quantum Dots Using Multiple Recombination Centers. *Phys. Rev. Lett.* **2009**, *103*, 207402.
22. Volkán-Kacsó, S.; Frantsuzov, P. A.; Jankó, B. Correlations between Subsequent Blinking Events in Single Quantum Dots. *Nano Lett.* **2010**, *10*, 2761–2765.
23. Frantsuzov, P. A.; Volkán-Kacscó, S.; Jankó, B. Universality of the Fluorescence Intermittency in Nanoscale Systems: Experiment and Theory. *Nano Lett.* **2013**, *13*, 402–408.
24. Ye, M.; Searson, P. C. Blinking in Quantum Dots: The Origin of the Grey State and Power Law Statistics. *Phys. Rev. B: Condens. Matter Mater. Phys.* **2011**, *84*, 125317.
25. Pelton, M.; Grier, D. G.; Guyot-Sionnest, P. Characterizing Quantum Dot Blinking Using Noise Power Spectra. *Appl. Phys. Lett.* **2009**, *85*, 819–821.
26. Schuster, J.; Cichos, F.; von Borczyskowski, C. Influence of Self-Trapped States on the Fluorescence Intermittency of Single Molecules. *Appl. Phys. Lett.* **2005**, *87*, 051915.
27. Schuster, J.; Cichos, F.; von Borczyskowski, C. Variation of Power-Law Dynamics Caused by Dark State Recovery of Fluorescence Intermittency of a Single Quantum System. *Proc. SPIE* **2006**, 625804.
28. Crouch, C. H.; Sauter, O.; Wu, X.; Purcell, R.; Querner, C.; Drudic, M.; Pelton, M. Facts and Artifacts in the Blinking Statistics of Semiconductor Nanocrystals. *Nano Lett.* **2010**, *10*, 1692–1698.
29. Watkins, L. P.; Yang, H. Detection of Intensity Change Points in Time-Resolved Single Molecule Measurements. *J. Phys. Chem. B* **2005**, *109*, 617–628.
30. Petrov, E. P.; Cichos, F.; von Borczyskowski, C. Intrinsic Photophysics of Semiconductor Nanocrystals in Dielectric Media: Formation of Surface States. *J. Lumin.* **2006**, *119−120*, 412–417.
31. Jones, M.; Lo, S. S.; Scholes, G. D. Quantitative Modelling of the Role of Surface Traps in CdSe/CdS/ZnS Nanocrystal Photoluminescence Decay Dynamics. *Proc. Natl. Acad. Sci. U. S. A.* **2009**, *106*, 3011–3016.
32. Al Salman, A.; Tortschanoff, A.; van der Zwan, G.; van Mourik, F.; Chergui, M. A Model for the Multi-Exponential Excited State Decay of CdSe Nanocrystals. *Chem. Phys.* **2009**, *357*, 96–101.
33. Knowles, K. E.; Mc Arthur, E. A.; Weiss, E. A. A Multi-Timescale Map of Radiative and Nonradiative Decay Pathways for Excitons in CdSe Quantum Dots. *ACS Nano* **2011**, *5*, 2026–2035.
34. Kern, S. J.; Sahu, K.; Berg, M. A. Heterogeneity of the Electron-Trapping Kinetics in CdSe Nanoparticles. *Nano Lett.* **2011**, *11*, 3493–3498.
35. Schlegel, G.; Bohnenberger, J.; Potapova, I.; Mews, A. Fluorescence Decay Time of Single Semiconductor Nanocrystals. *Phys. Rev. Lett.* **2002**, *88*, 1374011.
36. Fisher, B. R.; Eisler, H. J.; Stott, N.; Bawendi, M. G. Emission Intensity Dependence and Single-Exponential Behavior in Single Colloidal Quantum Dot Fluorescence Lifetimes. *J. Phys. Chem. B* **2004**, *108*, 143–148.
37. Biebricher, A.; Sauer, M.; Tinnefeld, P. Radiative and Nonradiative Rate Fluctuations of Single Colloidal Semiconductor Nanocrystals. *J. Phys. Chem. B* **2006**, *110*, 5174–5178.
38. Montiel, D.; Yang, H. Observation of Correlated Emission Intensity and Polarization Fluctuations in Single CdSe/ZnS Quantum Dots. *J. Phys. Chem. A* **2008**, *112*, 9352–9355.
39. Schmidt, R.; Krasselt, C.; von Borczyskowski, C. Change Point Analysis of Matrix Dependent Photoluminescence Intermittency of single CdSe/ZnS Quantum Dots with Intermediate Intensity Levels. *Chem. Phys.* **2012**, *406*, 9–14.
40. Knappenberger, K. L.; Wong, D. B.; Romanyuk, Y. E.; Leone, S. R. Excitation Wavelength Dependence of Fluorescence Intermittency in CdSe/ZnS Core/Shell Quantum Dots. *Nano Lett.* **2007**, *7*, 3869–3874.
41. Galland, C.; Ghosh, Y.; Steinbrück, A.; Sykora, M.; Hollingsworth, J. A.; Klimov, V. I. Two Types of Luminescence Blinking Revealed by Spectroelectrochemistry of Single Quantum Dots. *Nature* **2011**, *479*, 203–207.
42. Wang, X.; Ren, X.; Kahen, K.; Hahn, M. A.; Rajeswaran, M.; Maccagnano-Zacher, S.; Silcox, J.; Cragg, G. E.; Efros, A. L.; Krauss, T. D. Non-blinking Semiconductor Nanocrystals. *Nature* **2009**, *459*, 686–689.
43. Chon, B.; Lim, S. J.; Kim, W.; Seo, J.; Kang, H.; Joo, T.; Hwang, J.; Shin, S. K. Shell and Ligand-dependent Blinking of CdSe-based Core/Shell Nanocrystals. *Phys. Chem. Chem. Phys.* **2010**, *12*, 9312–9319.
44. Peterson, J. J.; Nesbit, D. J. Modified Power Law Behaviour in Quantum Dot Blinking: A Novel Role for Biexcitons and Auger Ionization. *Nano Lett.* **2009**, *9*, 338–345.

45. Stefani, F. D.; Knoll, W.; Kreiter, M.; Zhong, X.; Han, M. Y. Quantification of Photoinduced and Spontaneous Quantum Dot Luminescence Blinking. *Phys. Rev. B: Condens. Matter Mater. Phys.* **2005**, *72*, 125304.
46. Shimizu, K. T.; Neuhauser, R. G.; Leatherdale, C. A.; Empedocles, S. A.; Woo, W. K.; Bawendi, M. G. Blinking Statistics in Single Semiconductor Nanocrystal Quantum Dots. *Phys. Rev. B: Condens. Matter Mater. Phys.* **2001**, *63*, 205316.
47. Li, S.; Steigerwald, M. L.; Brus, L. E. Surface States in the Photoionization of High-Quality CdSe Core/Shell Nanocrystals. *ACS Nano* **2009**, *3*, 1267–1273.
48. Frenzel, J.; Joswig, J. O.; Seifert, G. Optical Excitations in Cadmium Sulfide Nanoparticles. *J. Phys. Chem. C* **2007**, *111*, 10761.
49. Kilina, S. V.; Ivanov, S.; Tretiak, S. Effect of Surface Ligands on Optical and Electronic Spectra of Semiconductor Nanoclusters. *J. Am. Chem. Soc.* **2009**, *131*, 7717–7726.
50. Kraus, R. M.; Lagoudakis, P. G.; Mueller, J.; Lupton, J. M.; Feldmann, J.; Talapi, D. V.; Weller, H. Interplay between Auger and Ionization Processes in Nanocrystal Quantum Dots. *J. Phys. Chem. B* **2005**, *109*, 18214–18217.
51. Gomez-Campos, F. M.; Califano, M. Hole Surface Trapping in CdSe Nanocrystals: Dynamics, Rate Fluctuations, and Implications for Blinking. *Nano Lett.* **2012**, *12*, 4508–4517.
52. Kambhampti, P. Hot Exciton Relaxation Dynamics in Semiconductor Quantum Dots: Radiationless Transitions on the Nanoscale. *J. Phys. Chem. C* **2011**, *115*, 22089–22109.
53. Blaudeck, T.; Zenkevich, E. I.; Cichos, F.; C. von Borczyskowski, C. Probing Wave Functions at Semiconductor Quantum-Dot Surfaces by Non-FRET Photoluminescence Quenching. *J. Phys. Chem. C* **2008**, *112*, 20251–20257.
54. Schapotschnikow, P.; Hommersom, B.; T. Vlugt, T. J. H. Adsorption and Binding of Ligands to CdSe Nanocrystals. *J. Phys. Chem. C* **2009**, *113*, 12690–12698.
55. Voznyy, O. Mobile Surface Traps in CdSe Nanocrystals with Carboxylic Acid Ligands. *J. Phys. Chem. C* **2011**, *115*, 15927–15932.